Radiation Constrained Wireless Charger Placement

Haipeng Dai*, Yunhuai Liu†, Alex X. Liu*, Lingtao Kong*, Guihai Chen*‡ and Tian He§¶
*State Key Laboratory for Novel Software Technology, Nanjing University, Nanjing, Jiangsu 210024, CHINA
†Third Research Institute of Ministry of Public Security, Shanghai, CHINA
‡Shanghai key Laboratory of Scalable Computing and Systems, Shanghai Jiao Tong University, Shanghai 200240, China
§Department of Automation, Shanghai Jiao Tong University, Shanghai 200240, China
¶Computer Science and Engineering, University of Minnesota, Minneapolis, MN 55455, USA
Emails: haipengdai@nju.edu.cn, yunhuai.liu@gmail.com, alexliu@nju.edu.cn,
michael.kong.nju@gmail.com, gchen@nju.edu.cn, tianhe@cs.umn.edu

***Abstract*—Wireless Power Transfer has become a commercially viable technology to charge devices because of the convenience of no power wiring and the reliability of continuous power supply. This paper concerns the fundamental issue of wireless charger placement with electromagnetic radiation (EMR) safety. Although there are a few wireless charging schemes consider EMR safety, none of them addresses the charger placement issue. In this paper, we propose PESA, a wireless charger Placement scheme that guarantees EMR SAfety for every location on the plane. First, we discretize the whole charging area and formulate the problem into the Multidimensional 0/1 Knapsack (MDK) problem. Second, we propose a fast approximation algorithm to the MDK problem. Third, we optimize our scheme to improve speed by double partitioning the area. We prove that the output of our algorithm is better than $(1-\epsilon)$ of the optimal solution to PESA with a smaller EMR threshold $(1-\epsilon/2)R_t$ and a larger EMR coverage radius $(1+\epsilon/2)D$. We conducted both simulations and field experiments to evaluate the performance of our scheme. Our experimental results show that in terms of charging utility, our algorithm outperforms the prior art by up to 45.7%.**

I. Introduction

Nowadays, Wireless Power Transfer (WPT) has become a commercially viable technology to charge devices due to its convenience of no power wiring and the reliability of continuous power supply. The Wireless Power Consortium established in 2008 has grown to include 211 members in 2015, including major IT leaders such as Microsoft and Samsung. A WPT system consists of some wireless chargers and rechargeable devices (such as WISP RFID tags [1] and rechargeable sensor nodes [2]). A wireless charger has a dedicated power source with significant power supply and can transfer power wirelessly to rechargeable devices. A rechargeable device is powered by harvesting the radio frequency energy from the chargers.

Notwithstanding the advantages the WPT technology offers, the high electromagnetic radiation (EMR) that goes along with this technology has caused more and more safety concerns for human health. High EMR exposure has been shown to associate with risks like tissue impairment [3], mental diseases [4] and brain tumor [5], and be even more dangerous to pregnant women and children [6], [7]. Due to concerns about adverse consequences of EMR exposure, exposure limits have been established in regulations like Title 47 of the Code of Federal Regulations (CFR) in the United States, Hygienic Standard for Environmental Electromagnetic Waves GB9175-88 [8] in China, and standards published by the International Commission on Non-Ionizing Radiation Protection (ICNIRP) [9] in most of Europe.

This paper considers the fundamental issue of wireless charger placement with human safety constraints on EMR. Given a set of geometrically deployed devices and a set of wireless chargers, we want to find locations to place the chargers so that the charging utility of all devices is maximized and there is no location where the aggregate EMR exceeds a given safety threshold for human beings. The charging utility of a device measures the amount of received power from multiple chargers. In other words, the higher the charging utility of a device, the more power it is charged. EMR safety here means that at any geometric location, the aggregate EMR from all nearby chargers needs to be lower than a threshold, beyond which is unsafe for human beings. Note that the aggregate EMR from multiple chargers has been shown to be the sum of each charger's EMR [10].

Though there have emerged some wireless charger placement schemes [11]–[13], none of them considers EMR safety. In addition, there is also some wireless charging work considering EMR safety [10], [14], but none of them addresses the charger placement issue. Existing wireless charger placement schemes cannot be easily adapted to address EMR safety because their schemes only work for specific scenarios due to strong assumptions. For example, the scheme proposed by He *et al.* only works for triangular topologies, where charger locations must form some equilateral triangles [11]; furthermore, it is unclear what approximation ratio that their scheme can achieve. The scheme proposed by Pang *et al.* uses an overly simplified charging model where the charging power of a charger is uniform within a disk coverage area [12]; however, in reality, the charging power of a charger is nearly inversely proportional to the square of the distance.

The problem of wireless charger placement with EMR safety has three key challenges. First, the number of locations that we can place chargers is infinite. Second, the number of locations that we need to guarantee EMR safety is also infinite. Third, the two problems of placing chargers and guaranteeing EMR safety are tightly coupled and cannot be solved separately.

In this paper, we propose a wireless charger Placement scheme that guarantees EMR SAfety for every location on the

978-1-4673-9953-1/16/$31.00 ©2016 IEEE

plane (PESA). First, we discretize the whole charging area such that the problem can be formulated into the Multidimensional 0/1 Knapsack (MDK) problem. Second, as existing MDK approximation algorithms are not optimized for speed, we propose a fast approximation algorithm to the MDK problem. Third, we optimize our charger placement scheme to further improve speed by double partitioning the area.

Our scheme addresses the first two challenges by area discretization. Area discretization not only makes the number of locations to be finite, but also allows us to flexibly adjust the discretization granularity to achieve required optimality. The finer grained the area discretization is, the closer that our solution is to the optimal charger placement. Our scheme addresses the third challenge by formulating our problem as an integer programming problem, *i.e.*, formulating the EMR safety as linear constraints; thus, the calculated solution to the integer programming problem addresses both charger placement and EMR safety at the same time. Comparing our work with prior wireless charger placement schemes, unlike [11], [13], we assume that chargers can be placed at any location on our discretized area and the discretization can be arbitrarily fine grained; unlike [12], we adopt the realistic charging model in which charging power is nearly inversely proportional to the square of the distance.

In this paper, we make the following four key contributions. First, we formulate the problem of wireless charger placement with EMR safety. This paper represents the first step on addressing this problem. Second, we propose an area discretization approach to reformulate the above problem into a traditional MDK problem. We also propose a fast MDK approximation algorithm. Third, we propose a double partition method to further improve the speed of our MDK approximation algorithm. We prove that the output of our algorithm is better than $(1-\epsilon)$ of the optimal solution to PESA with a smaller EMR threshold $(1-\epsilon/2)R_t$ and a larger EMR coverage radius $(1+\epsilon/2)D$, where D is the EMR coverage radius of chargers. Fourth, we implemented our scheme in both Matlab and TX91501 power transmitters, and conducted both simulations and field experiments to evaluate the performance of our PESA scheme. Our results show that in terms of charging utility, our algorithm outperforms the prior art (*i.e.*, the algorithm in [11]) by up to 45.7%.

The rest of the paper proceeds as follows. We first review related work in Section II. Then, we present our problem statement in Section III, basic scheme in Section IV, and optimized scheme in Section V. In Sections VI and VII, we present our simulation results and field experimental results, respectively. We conclude the paper in Section VIII.

II. Related Work

Some wireless charger placement schemes have been proposed [11]–[13], but none of them considers EMR safety. He *et al.* proposed a wireless charger placement scheme where chargers must form equilateral triangles. Their optimization goal is to minimize the edge length of these triangles. Zhang *et al.* studied the joint optimization problem of charger placement and power allocation. They assumed that chargers can only be placed at a given set of candidate locations, and the aggregate power of chargers is subject to a power budget. Their objective is to maximize the overall charging utility. Pang *et al.* proposed a scheme to minimize the number of wireless chargers for charging a set of sensors placed in a two dimensional region [12]. They used the charging model of a charger's charging power being uniform within a disk coverage area. However, this charging model is overly simplified. In practice, a charger's charging power is nearly inversely proportional to the square of the distance [11], [15].

Some wireless charging work considers EMR safety [10], [14], but none of them addresses the charger placement issue. For example, Dai *et al.* proposed a charging efficiency optimization scheme that considers EMR safety [10]. Specifically, Dai's scheme turns on/off statically deployed chargers to achieve the maximum charging utility while guaranteeing that no location has EMR exceeding a given threshold.

TABLE I
Notations

Symbol	Meaning
s_i, S	Charger i, charger set
n	Number of chargers
o_j, O	Device j, device set
m	Number of devices
Ω	Area interested
$P(d)$	Received power from distance d
D	Farthest distance a charger can reach
δ	Gridding granularity
$d(s_i, o_j)$	Distance from charger s_i to device o_j
$d(s_i, p)$	Distance from charger s_i to point p
$u(o_j)$	Charging utility of device o_j
$e(d)$, $e(p)$	EMR from distance d, EMR at a point p
R_t	Hard threshold of EMR safety

III. Problem Statement

In this section, we first introduce our system modeling and then formally formulate our problem of wireless charger placement with EMR safety. Table I shows our notations.

A. System Modeling

Let $O = \{o_1, o_2, \ldots, o_m\}$ be the set of m rechargeable devices randomly placed on a two-dimensional region Ω. Let $S = \{s_1, s_2, \ldots, s_n\}$ be the n given wireless chargers [16]–[18] that are used to power up the m devices.

For the charging model of a charger and a device, we use the following model that has been validated in prior work [10]:

$$P(d) = \begin{cases} \frac{\alpha}{(d+\beta)^2}, & d \le D \\ 0, & d > D \end{cases} \tag{1}$$

where d is the distance between the device and the charger, α and β are constants determined by the hardware characteristics of the charger and the device as well as the surrounding environment, and D is the radius of the disk-shaped charging area of the charger. For the charging model of multiple chargers, we use the widely adopted model that the wireless power received by a device is the sum of the power that the device receives from every charger [10], [11].

For the charging utility model, we use the following model employed in prior wireless charging work [10], [14]: the charging utility is proportional to the charging power, *i.e.*

$$u(o_j) = C_1 \sum_{i=1}^{n} P(d(s_i, o_j)) \tag{2}$$

where $d(s_i, o_j)$ is the distance from the charger s_i to the device o_j, and C_1 is a constant.

For the EMR model, we use the following model validated in [10]: the intensity of EMR is proportional to the received power there, *i.e.*,

$$e(d) = C_2 P(d) \tag{3}$$

where d is the distance and C_2 is the constant to capture the linear relationship. Similarly to the charging model of multiple chargers, we model the EMR of multiple chargers to be additive. That is, the aggregated EMR at a location p is

$$e(p) = \sum_{i=1}^{n} e(d(s_i, p)) = C_2 \sum_{i=1}^{n} P(d(s_i, p)). \tag{4}$$

B. Problem Formulation

To guarantee the EMR safety over the field interested, we set up an EMR threshold R_t and require that the EMR intensity at any point p in the field should not exceed R_t. Based on Eq. 4, we mathematically express this EMR requirement as

$$\forall p \in \mathbb{R}^2, \quad C_2 \sum\nolimits_{i=1}^{n} P(d(s_i, p)) \leq R_t.$$

Our goal is to maximize the overall charging utility from all devices, *i.e.*, $\sum_{j=1}^{m} u(o_j)$. By Eq. 2, we have

$$\sum\nolimits_{j=1}^{m} u(o_j) = C_1 \sum\nolimits_{j=1}^{m} (\sum\nolimits_{i=1}^{n} P(d(s_i, o_j))). \tag{5}$$

Let p_{s_i} denote the location of the charger s_i. The wireless charger Placement with EMR SAfety (PESA) problem can thus be defined as follows

$$\begin{aligned} \textbf{(P1)} \quad \max \quad & C_1 \sum\nolimits_{j=1}^{m} (\sum\nolimits_{i=1}^{n} P(d(s_i, o_j))) \\ \textit{s.t.} \quad & \forall p \in \mathbb{R}^2, \quad C_2 \sum\nolimits_{i=1}^{n} P(d(s_i, p)) \leq R_t, \\ & p_{s_i} \in \Omega \qquad (i = 1, 2, \ldots, n). \end{aligned} \tag{6}$$

IV. The Basic Scheme

In this section, we propose a basic scheme to address PESA. We first introduce an area gridding method to reduce the number of candidate locations of chargers and the number of constraints in **P1** from infinite to finite. Then, we reformulate our problem into a traditional multidimensional 0/1 knapsack problem and present a near optimal solution.

A. Area Discretization

First, we try to confine the area of charger placement. As illustrated in Fig. 1(a), the green rectangular area denotes the area where the devices are located, which we call the *device area*. As a charger covers a disk region with radius D, we only need to consider the area obtained by uniformly expanding the device area by D along horizontal and vertical directions for charger placement, since deployed chargers out of this region would fail to cover any device (more precisely, the placement region for chargers is a rounded rectangle, we use a rectangle here for ease of analysis). We call this area the *placement area* associated with the device area.

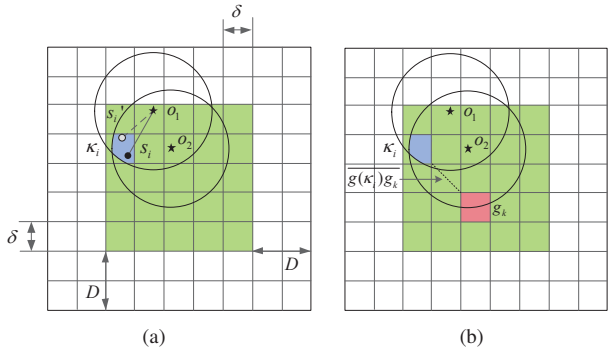

Fig. 1. Illustration of area discretization, and power and EMR approximation

Next, to address the main challenges raised by the infinite solution space for charger placement and the EMR requirement at any point on the plane, we propose to partition the placement area into small subareas and specify one point in each subarea for charger placement, and then apply different approximation schemes for charging power and EMR.

Basically, for area discretization we first discretize the area into uniform grids with side length of δ, and then further divide the subareas by drawing circles with radius D for each device. For example, in Fig. 1(a), there are 81 subareas after gridding and 33 more after drawing circles. Suppose we obtain Γ number of subareas and denote them by $\kappa_i\,(i = 1, 2, \ldots, \Gamma)$, and Γ_g number of grids $g_i\,(i = 1, 2, \ldots, \Gamma_g)$. Next, we randomly choose a point in each subarea as the candidate placement position for chargers. This is essentially a means to approximate any possible placement scheme. For instance, for a scheme with a placed charger s_i in κ_i, as shown in a black circle in Fig. 1(a), we approximate it with the charger s_i' shown in a grey circle. *We emphasize that in each subarea it is allowed to place more than one chargers, given that the EMR safety is not violated.*

The distances from each charger to devices are approximated accordingly. For instance, the distance from the charger s_i to a device o_1, *i.e.* $d(s_i, o_1)$, is approximated as $d(s_i', o_1)$, as illustrated in black solid and dotted lines, respectively. This will finally result in the approximation of received power of devices. Further, we emphasize that original distance and approximated distance should be either both bigger than D or both not. Otherwise, a nonzero charging power will be approximated by a zero power or vice versa, and thus leads to unbounded approximation error. This is why we need to further partition the subareas by drawing circles for devices. For example, both of the chargers s_i and s_i' in κ_i have nonzero charging power to devices o_1 and o_2.

We have the following lemmas for the number of obtained subareas after area discretization as well as charging power approximation error. Due to space limit, we omit most of the proofs of the lemmas and theorems in this paper.

Lemma 1. The obtained number of subareas Γ after area discretization is $O(\frac{|\Omega|}{\delta^2} + \frac{n^2 D}{\delta})$, where $|\Omega|$ denotes the size of the area interested, δ is the side length of grids.

Lemma 2. Setting δ as $\delta = \frac{\sqrt{2}}{2}\beta(\frac{1}{\sqrt{1-\epsilon}} - 1)$ where ϵ is an arbitrarily small positive value, we have the approximation error of charging power as $P(d(s_i', o_j)) \geq (1-\epsilon)P(d(s_i, o_j))$.

We proceed to study how to approximate the EMR value. Specifically, we approximately view the EMR value originated from a charger at any location in a subarea κ_i to any point inside a grid g_k as a constant, which is equivalent to that achieved from a distance equaling to *the shortest distance $\overline{g(\kappa_i)g_k}$ between the two grids $g(\kappa_i)$ and g_k that the charger and the point located in, where $g(\kappa_i)$ denotes the grid that contains κ_i*. Taking Fig. 1(b) as an example, the EMR value from a charger in a subarea κ_i to any point in a grid g_k is regarded as constant, and the EMR approximation distance is $\overline{g(\kappa_i)g_k}$, the shortest distance between the grids $g(\kappa_i)$ and g_k as shown in gray dotted line. Apparently, the approximated EMR value is the maximum EMR value that can be achieved by any charger and any point in the given two grids.

Besides, for the coverage distance of chargers under EMR approximation (*i.e.*, at which distance a grid receives a nonzero EMR from a charger in a subarea), we adopt a conservative scheme which decides the coverage distance by checking whether $\overline{g_i g_k}$ exceeds D or not. This will lead to a more stringent constraint in our reformulated problem, which helps to guarantee the EMR safety after the EMR approximation.

To sum up, we use the following equation to approximate the EMR from a charger in subarea κ_i to grid g_k:

$$\varepsilon(\kappa_i g_k) = \begin{cases} \frac{C_2\alpha}{(\overline{g(\kappa_i)g_k}+\beta)^2}, & \overline{g(\kappa_i)g_k} \le D \\ 0, & \overline{g(\kappa_i)g_k} > D \end{cases} \tag{7}$$

We have the following lemmas for the EMR coverage distance approximation and EMR approximation error.

Lemma 3. If $\varepsilon(\kappa_i g_k) > 0$, which means that the approximated EMR from a charger in subarea κ_i to grid g_k is greater than zero, then any point in g_k must be covered by a charger at any location in κ_i with an EMR coverage distance $D + 2\sqrt{2}\delta$.

Lemma 4. Let $e(p)$ be the EMR at a point p inside a grid g_i from a charger in a subarea κ_i, $\varepsilon(\kappa_i g_k)$ be the approximated EMR from κ_i to g_i. Setting δ as $\delta = \frac{\sqrt{2}}{4}\beta(\frac{1}{\sqrt{1-\epsilon}} - 1)$ where ϵ is an arbitrarily small positive value, we have the EMR approximation error as $e(p) \le \varepsilon(\kappa_i g_k) \le \frac{e(p)}{1-\epsilon}$.

B. Problem Reformulation and Solution

After the above approximation procedures, we can express the EMR requirement in each subarea as a constraint, and thereby reduce the number of constraints in **P1** from infinite to finite. We use a binary indicator $x_i^h, h = (1, \ldots, n)$ to denote whether the h-th charger in i-th subarea is switched on or not. PESA can thus be reformulated as

$$\textbf{(P2)}\ \max\ C_1 \sum_{j=1}^{m}\sum_{i=1}^{\Gamma}(\sum_{h=1}^{n} P(d(s_i', o_j))x_i^h)$$

$$s.t.\ \sum_{i=1}^{\Gamma}\sum_{h=1}^{n} \varepsilon(\kappa_i g_k)x_i^h \le R_t, (k = 1, \ldots, \Gamma_g) \tag{8}$$

$$\sum_{i=1}^{\Gamma}\sum_{h=1}^{n} x_i^h \le n,$$

$$x_i^h \in \{0, 1\}\,(i = 1, \ldots, \Gamma; h = 1, \ldots, n). \tag{9}$$

Note that in each subarea we can put at most n chargers. This is a typical Multidimensional 0/1 Knapsack (MDK) problem [22]. However, as the number of constraint is greater than 2, there does not exist an FPTAS (Fully Polynomial-Time Approximation Scheme) unless $P = NP$ according to the classical results in [22]. We thus develop a near optimal algorithm to address this issue as shown in Algorithm 1.

Algorithm 1 Near Optimal Algorithm for the Reformulated PESA Problem

INPUT The position of each device, the number of chargers n, the parameters of the charging model and the utility model α, β, C_1, C_2, EMR threshold R_t and error threshold ϵ.

OUTPUT The near optimal placement scheme and its charging utility U^*.

1: Let $\epsilon_1 = \min\{\epsilon/2, \frac{1}{n+2}\}$ and $\epsilon_2 = \epsilon - \epsilon_1$;

2: Partition the associated placement area of the device area into multiple subareas by drawing uniform grids with side length $\delta = \min\{\frac{\sqrt{2}}{4}\beta(\frac{1}{\sqrt{1-\epsilon_2}} - 1), \frac{\sqrt{2}}{4}\epsilon_2 D\}$ and circles for each device with radius D, and derive the corresponding MDK problem.

3: Conduct redundant constraint reduction approaches proposed in [19], [20] and [21] for the MDK problem, and still use Γ_g to denote the obtained number of constraints if no confusion arises.

4: Let $w_{ih}^k = \varepsilon(\kappa_i g_k)$ $(k = 1, 2, \ldots, \Gamma_g)$ and $w_{ih}^{\Gamma_g+1} = 1$ denote the coefficient of x_i^h in Eq. 8 and Eq. 9, respectively. Constructing a new MDK instance by defining

$$w_{ih}^{k'} = \lfloor \frac{w_{ih}^k}{R_t}\frac{n\Gamma}{\epsilon_1} \rfloor + 1, (k = 1, 2, \ldots, \Gamma_g) \tag{10}$$

$$w_{ih}^{\Gamma_g+1'} = \lfloor \frac{(1-\epsilon_1)w_{ih}^{\Gamma_g+1}}{n}\frac{n\Gamma}{\epsilon_1} \rfloor + 1, \tag{11}$$

$$R_t' = \lfloor \frac{n\Gamma}{\epsilon_1} \rfloor, \tag{12}$$

$$n' = \lfloor \frac{n\Gamma}{\epsilon_1} \rfloor, \tag{13}$$

5: Use traditional dynamic programming to compute the solution x_i^h of the constructed MDK instance.

6: Output U^* and its corresponding placement scheme.

It is worthwhile to mention that we apply three redundant constraint reduction approaches, namely bounds method [19], linear programming method [20] and heuristic method [21], to eliminate the redundant constraints in the MDK problem at Step 3 in order to reduce the computational effort at Step 5. Here redundant constraints refer to those constraints whose presence does not change the optimum solution. By this means we can substantially reduce the computational cost in the next stages. The following theorem indicates the theoretical performance of Algorithm 1.

Theorem 1. The output of Algorithm 1 is a feasible solution to the original PESA problem, and is better than $(1-\epsilon)$ of the optimal solution to PESA with a smaller EMR threshold $(1-\epsilon)R_t$ and a larger EMR coverage radius $(1+\epsilon)D$. In addition, the time complexity of Algorithm 1 is $O(\frac{n}{\epsilon^2}(|\Omega| + \epsilon n^2)(\frac{n}{\epsilon^3}(|\Omega| + \epsilon n^2))^{\Gamma_g+1})$ where $|\Omega|$ is the size of device area, Γ_g is the number of constraints obtained after redundant constraint reduction except the cardinality constraint (in the worst case, $\Gamma_g = O(\frac{|\Omega|}{\epsilon^2})$).

Proof: First of all, as we set $\delta = \min\{\frac{\sqrt{2}}{4}\beta(\frac{1}{\sqrt{1-\epsilon_2}} - 1), \frac{\sqrt{2}}{4}\epsilon_2 D\}$, we have the EMR approximation $\varepsilon(\kappa_i g_k) \le \frac{e(p)}{1-\epsilon_2}$ by following Lemma 4, the approximation error of charging power as $P(d(s_i', o_i)) \ge (1-\epsilon_2)P(d(s_i, o_i))$ by following

Lemma 2, and the fact that any point in g_k must be covered by a charger at any location in κ_i with an EMR coverage distance $(1+\epsilon_2)D$ by following Lemma 3. Thus we can prove that the optimal solution to the problem **P2** must outperform $(1-\epsilon_2)$ of the optimal solution to the PESA with a smaller EMR threshold $(1-\epsilon_2)R_t$ and a larger EMR coverage radius $(1+\epsilon_2)D$.

Furthermore, we claim that the redundant constraint reduction approaches [19]–[21] designed for linear programming and performed at Step 3 can also apply to the integer linear programming problem **P2**. This is because the solution space of the integer linear programming problem must be contained by that of the linear programming problem. As the latter one won't change after applying the reduction approaches, so does the former one. We thus have the following lemma.

Lemma 5. Redundant linear constraint reduction methods for linear programming can apply to integer linear programming.

Next, at Step 4 we construct a new MDK instance and solve it at Step 5. We will prove that the output of Algorithm 1, x_i^h, outperforms the optimal solution to **P2** with a relaxed EMR threshold $(1-\epsilon_1)R_t$. Firstly, we will prove that x_i^h is a feasible solution to **P2**. According to Eq. 10, 11, 12 and 13, we have

$$\sum_{n\Gamma} w_{ih}^k x_i^h < \frac{\epsilon_1 R_t}{n\Gamma} \sum_{n\Gamma} w_{ih}^{k'} x_i^h \leq \frac{\epsilon_1 R_t}{n\Gamma} \lfloor \frac{n\Gamma}{\epsilon_1} \rfloor \leq R_t \qquad (14)$$

$(k = 1, 2, \ldots, \Gamma_g)$, and

$$\sum_{n\Gamma} w_{ih}^{\Gamma_g+1} x_i^h < \frac{\epsilon_1 n}{(1-\epsilon_1)n\Gamma} \sum_{n\Gamma} w_{ih}^{\Gamma_g+1'} x_i^h \leq \frac{\epsilon_1 n}{(1-\epsilon_1)n\Gamma} \lfloor \frac{n\Gamma}{\epsilon_1} \rfloor \leq \frac{n}{1-\epsilon_1}. \qquad (15)$$

As $\epsilon_1 = \min\{\epsilon/2, \frac{1}{n+2}\}$, we have $\lfloor \frac{n}{1-\epsilon_1} \rfloor \leq \lfloor \frac{n+2}{n+1} n \rfloor = n$. Since $\sum_{n\Gamma} w_{ih}^{\Gamma_g+1} x_i^h$ is an integer, Eq. 15 also implies $\sum_{n\Gamma} w_{ih}^{\Gamma_g+1} x_i^h \leq n$.

We will proceed to show that any solution $x_i^{h'}$ to the problem **P2** with a relaxed EMR threshold $(1-\epsilon_1)R_t$ also satisfy the constructed instance. For $x_i^{h'}$, we have $\sum_{n\Gamma} w_{ih}^k x_i^j \leq (1-\epsilon_1)R_t$ and $\sum_{n\Gamma} w_{ih}^{\Gamma_g+1} x_i^{h'} \leq n$. Combined with Eqs. 10 and 11, we have

$$\sum_{n\Gamma} w_{ih}^{k'} x_i^{h'} \leq \frac{n\Gamma}{\epsilon_1 R_t} \sum_{n\Gamma} w_{ih}^k x_i^{h'} + \sum_{n\Gamma} x_i^{h'} \leq \frac{n\Gamma}{\epsilon_1 R_t}(1-\epsilon_1)R_t + n\Gamma \leq \frac{n\Gamma}{\epsilon_1}, \qquad (16)$$

$(k = 1, 2, \ldots, \Gamma_g)$, and

$$\sum_{n\Gamma} w_{ih}^{\Gamma_g+1'} x_i^{h'} \leq \frac{(1-\epsilon_1)n\Gamma}{\epsilon_1 n} \sum_{n\Gamma} w_{ih}^{\Gamma_g+1} x_i^{h'} + \sum_{n\Gamma} x_i^{h'} \leq \frac{(1-\epsilon_1)n\Gamma}{\epsilon_1 n} n + n\Gamma \leq \frac{n\Gamma}{\epsilon_1}, \qquad (17)$$

Since $\sum_{n\Gamma} w_{ih}^{k'} x_i^{h'}$ and $\sum_{n\Gamma} w_{ih}^{\Gamma_g+1'} x_i^{h'}$ are integers, we have $\sum_{n\Gamma} w_{ih}^{k'} x_i^{h'} \leq \lfloor \frac{n\Gamma}{\epsilon_1} \rfloor$ and $\sum_{n\Gamma} w_{ih}^{\Gamma_g+1'} x_i^{h'} \leq \lfloor \frac{n\Gamma}{\epsilon_1} \rfloor$.

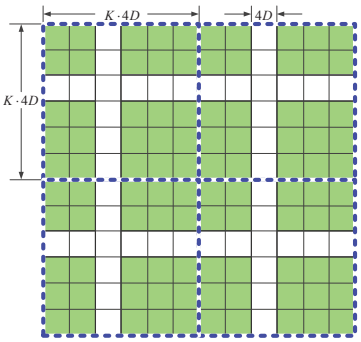

Fig. 2. Illustration of overall partition

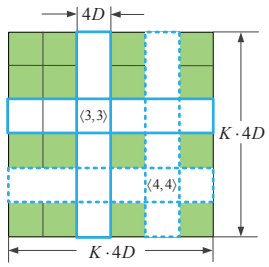

Fig. 3. Illustration of K-$Grid$

As x_i^h is the optimal solution to the constructed MDK instance, we claim that x_i^h must outperform the optimal solution to the problem **P2** with a relaxed EMR threshold $(1-\epsilon_1)R_t$. Combined with the former analysis, we can prove that the output of Algorithm 1 outperforms $(1-\epsilon_2)$ of the optimal solution to the PESA with a smaller EMR threshold $(1-\epsilon_1)(1-\epsilon_2)R_t$ and a larger EMR coverage radius $(1+\epsilon_2)D$, and thus outperforms $(1-\epsilon)$ of the optimal solution to PESA with a smaller EMR threshold $(1-\epsilon)R_t$ and a larger EMR coverage radius $(1+\epsilon)D$.

Apparently, the output is a feasible solution to the original PESA problem. To save space, we omit the analysis of the time complexity. ■

We emphasize that performing Step 4 and Step 5 in Algorithm 1 rather than the traditional polynomial time approximation scheme to MDK can help reduce the time complexity from $O((n\Gamma)^{\lceil \frac{(\Gamma_g+1)}{\epsilon} \rceil - (\Gamma_g+1)})$ to $O(n\Gamma(\frac{n\Gamma}{\epsilon})^{\Gamma_g+1})$. In addition, it can be seen that the number of constraints Γ_g plays an important role in the time complexity, this is exactly why we need to reduce the constraints as much as possible.

By Theorem 1, the time complexity of Algorithm 1 rises exponentially with Γ_g that is proportional to the size of device area $|\Omega|$ in the worst case, making Algorithm 1 prohibitively expensive for most applications. To this end, we will discuss how to optimize the basic scheme in the next section.

V. The Optimized Scheme

In this section, we propose an optimized scheme to reduce the computational effort of the basic scheme. Particularly, we first introduce the basic idea of our scheme which is based on double partition, and then boil down the converted problem into two subproblems, and address them respectively.

A. Key Idea of Double Partition Scheme

Generally speaking, our optimized scheme follows the spirit of the divide-and-conquer strategy, and more precisely, it can be classified into the double partition methods [23]. We artificially divide the whole area into multiple separate subareas such that we can safely consider the charger placement problem with EMR safety in each of them independently. Next, with the given budget of chargers, we need to intelligently determine the number of placed chargers in each subarea in order to maximize the overall charging utility. As a result, the central issue of our problem becomes how to divide the whole area, assign chargers to the obtained subareas and place them.

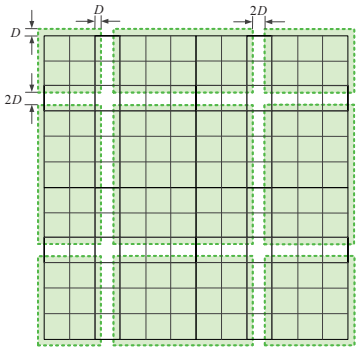

Fig. 4. Illustration of placement areas after adopting policy $< 3, 3 >$

Fig. 2 shows an example of area division. First of all, we divide the whole device area into uniform $4D * 4D$ squares. Then we group $K * K$ such squares into larger squares, which we call K-$Grid$s. In Fig. 2, we set $K = 6$ and thus get 4 K-$Grid$s. For convenience of analysis, we assume without loss of generality that the whole area can be partitioned into an integral number of K-$Grid$s (if it is not the case, we can add phantom $4D * 4D$ squares to achieve this goal).

Considering the EMR originated from the deployed chargers in neighboring K-$Grid$s, it is obviously not safe to investigate the charger placement problem for every K-$Grid$ separately. Instead, we use the following technique to decompose the charger placement problem. As Fig. 2 illustrates, we force each K-$Grid$ to adopt the same device-erasure policy. That is, we equivalently regard that the devices located in the i-th row and j-th column are "removed". Formally, we use a two-tuple $< i, j >$ to denote such policy. Fig. 3 demonstrates two policies, *i.e.*, $< 3, 3 >$ and $< 4, 4 >$, and Fig. 2 shows the result when all K-$Grid$s adopt policy $< 3, 3 >$.

Consequently, the whole area is partitioned into multiple (say $\mathcal{N}$) subareas, each of which contains no more than $(K-1) * (K-1)$ squares. Moreover, the distance between any pair of subareas is no smaller than $4D$. For instance, Fig. 2 has 9 partitioned subareas, and the biggest one contains $5*5$ squares. We name these newly formed subareas $(K-1)$-$Grid$s. Furthermore, we claim that the distance of $4D$ is enough to eliminate the dependency of placement scheme determination between adjacent subareas. To see this, we take a closer look at the placement area of chargers for each subarea. As stated in Sec. IV.A, it is exactly the dilated rectangular subarea with a dilated distance of D. Fig. 4 demonstrates the placement area for each subarea in Fig. 2. As a result, the minimum distance of $2D$ between the adjacent placement areas for chargers ensures that there is no EMR coming from chargers in neighboring placement areas, and we can apply Algorithm 1 for each area with a given number of chargers to obtain a near optimal placement scheme.

Till now, our problem is boiled down to two subproblems. One is given a device-erasure policy, how to assign the chargers to each subarea and further determine their locations to maximize the overall charging utility. The other is how to determine the device-erasure policy which yields the maximum overall charging utility. We deal with these two subproblems in the following two subsections respectively.

Algorithm 2 Dynamic Algorithm for Global Solution Construction

INPUT The position of each device, the number of chargers n, the parameters of the charging model and the utility model α, β, C_1, C_2, EMR threshold R_t, error threshold ϵ and a given device-erasure policy.

OUTPUT Assigned number of chargers for each $(K-1)$-$Grid$, the overall charging utility U.

1: Apply Algorithm 1 with error threshold ϵ and p $(p = 1, 2, \ldots, n)$ number of chargers for each i-th $(K-1)$-$Grid$ $(i = 1, 2, \ldots, \mathcal{N})$ for the given policy, and obtain the charging utility, say U_i^p;
2: Let $U(1)$, $U(2)$,..., $U(n)$ store the current maximum overall charging utility with 1, 2, ..., n chargers, respectively;
3: **for** the i-th $(K-1)$-$Grid$ $(i = 1, 2, \ldots, \mathcal{N})$ **do**
4: **for** $U(j)$ $(j = 1, 2, \ldots, n)$ **do**
5: Update $U(j)$ as $U(j) = \max_{p=(0,1,2,\ldots,j)}\{U(j-p)+U_i^p\}$, and record the assigned number of chargers and their placed locations of each subarea for $U(j)$;
6: **end for**
7: **end for**
8: Output $U(n)$ and its corresponding assigned number of chargers of each subarea.

Algorithm 3 Near Optimal Algorithm for PESA

INPUT The position of each device, the number of chargers n, the parameters of the charging model and the utility model α, β, C_1, C_2, EMR threshold R_t and error threshold ϵ.

OUTPUT the optimal placement scheme and its charging utility $U^{\#}$.

1: Partition the device area into multiple $4D*4D$ squares, and group $K * K$ such squares to form K-$Grid$s where $K = \frac{1}{1-\sqrt{1-\epsilon/2}}$.
2: Apply Algorithm 2 to compute the overall charging utility for all possible K^2 policies with error threshold $\epsilon/2$, and find the largest one $U^{\#}$ and record the corresponding placement scheme.
3: Output $U^{\#}$ and its corresponding placement scheme.

B. Near Optimal Placement Scheme under a Given Area Partition Scheme

Suppose that after applying Algorithm 1, the obtained near optimal utility for the i-th $(K-1)$-$Grid$ $(i = 1, \ldots, \mathcal{N})$ provided with p $(p = 1, \ldots, n)$ number of chargers is U_i^p. Now, our task is to construct a global feasible solution based on this information. This can be done by employing a dynamic programming method as illustrated in Algorithm 2, for which we have the following theorem.

Theorem 2. The output of Algorithm 2 is a feasible solution to the original PESA problem under the given area partition scheme, and is better than $(1-\epsilon)$ of the optimal solution to PESA with a smaller EMR threshold $(1-\epsilon)R_t$ and a larger EMR coverage radius $(1+\epsilon)D$.

C. Double Partition Scheme and Performance Analysis

The details of our double partition scheme are presented in Algorithm 3. In general, the double partition scheme simply searches all possible device-erasure policies for the "best" one that yields the optimal overall charging utility. The following theorem describes the performance of Algorithm 3.

Theorem 3. The output of Algorithm 3 is a feasible solution to the original PESA problem, and is better than $(1-\epsilon)$ of the optimal solution to PESA with a smaller EMR threshold $(1-\epsilon/2)R_t$ and a larger EMR radius $(1+\epsilon/2)D$. In addition, the time complexity of Algorithm 3 is $O(|\Omega|\frac{n^2}{\epsilon^4}(1+$

$\frac{\epsilon n^2}{A})(\frac{n}{\epsilon^3}(A+\epsilon n^2))^{\Gamma_g+1})$ where $A = O(\frac{1}{\epsilon^2})$, $|\Omega|$ is the size of device area, Γ_g is the number of constraints obtained after redundant constraint reduction except the cardinality constraint for subareas.

Proof: Let U^* denote the charging utility of the optimal solution to PESA with a smaller EMR threshold $(1-\epsilon/2)R_t$ and a larger EMR coverage radius $(1+\epsilon/2)D$, and $U^*_{<i,j>}$ the corresponding charging utility obtained by switch on the chargers located in the placement areas for policy $< i,j >$ while switching off the others for the optimal solution. In addition, let $U^{OPT}_{<i,j>}$ denote the optimal solution to PESA adopting policy $< i,j >$ with a smaller EMR threshold $(1-\epsilon/2)R_t$ and a larger EMR coverage radius $(1+\epsilon/2)D$. Obviously, we have $U^*_{<i,j>} \leq U^{OPT}_{<i,j>}$. By following Theorem 2, the output charging utility of Algorithm 2 for policy $< i,j >$, say $U^{\#}_{<i,j>}$, is subject to

$$U^{\#}_{<i,j>} \geq (1-\epsilon/2)\cdot U^{OPT}_{<i,j>} \geq (1-\epsilon/2)\cdot U^*_{<i,j>}. \quad (18)$$

Now, let's consider the summation of $U^{\#}_{<i,j>}$ for all possible policies. We have

$$\sum_{i=1}^{K}\sum_{j=1}^{K} U^{\#}_{<i,j>} \geq \sum_{i=1}^{K}\sum_{j=1}^{K}(1-\epsilon/2)\cdot U^*_{<i,j>}. \quad (19)$$

Next, we have a critical observation that $\sum_{i=1}^{K}\sum_{j=1}^{K} U^*_{<i,j>} \geq (K^2-2K+1)U^*$ (it can be verified by the truth that each charger in U^* must be located in the placement areas for more than (K^2-2K+1) policies). We therefore obtain

$$\sum_{i=1}^{K}\sum_{j=1}^{K} U^{\#}_{<i,j>} \geq (1-\epsilon/2)(K^2-2K+1)U^*. \quad (20)$$

Moreover, since the output of Algorithm 3, $U^{\#}$, is the largest one among all $U^{\#}_{<i,j>}$, we thus have

$$\begin{aligned} U^{\#} &\geq \frac{1}{K^2}\sum_{i=1}^{K}\sum_{j=1}^{K} U^{\#}_{<i,j>} \geq (1-\epsilon/2)\frac{K^2-2K+1}{K^2}U^* \\ &\geq (1-\epsilon/2)(1-\epsilon/2)U^*_{<i,j>} \geq (1-\epsilon)U^*. \end{aligned} \quad (21)$$

To save space, we omit the analysis of the solution's feasibility and its time complexity. ■

As stated in Theorem 3, the time complexity of Algorithm 3 is exactly proportional to the size of the device area $|\Omega|$, which means Algorithm 3 is scalable and is far more efficient than Algorithm 1 whose time complexity rises exponentially with $|\Omega|$. Besides, though the running time of Algorithm 3 still grows exponentially with ϵ, using redundant constraint reduction approaches at Step 3 in Algorithm 1 can substantially reduce the running time. Moreover, we employ *pruning techniques* when implementing this algorithm to further speed up the computation. We omit the details to save space.

VI. Simulation Results

In this section, we present simulation results to evaluate the performance of our algorithms in terms of error threshold ϵ, EMR threshold R_t, charger number and device number. We also provide insights about why our algorithm achieves a high charging gain.

A. Evaluation Setup

Unless otherwise stated, we use the following default parameter setup in the simulation. Suppose we have 50 devices distributed on a $20\,m * 20\,m$ area, and 20 chargers to be deployed. For charging model and EMR model, we set $\alpha = 10$, $\beta = 10$, $D = 4$, $C_1 = C_2 = 1$. In addition, the error threshold is set to $\epsilon = 0.8$ and the EMR threshold is set to $R_t = 0.4$.

B. Baseline Setup

As there is no algorithm available for charger placement with EMR concern, we devise two algorithms, namely random algorithm and triangular placement algorithm, for comparison.

At each round, the random algorithm randomly places a charger on the placement area, and checks whether the EMR safety constraint is satisfied by discretizing the whole area into fine-grained grids and computing the EMR intensity at the central point of each grid. If not, the algorithm randomly chooses another location for charger placement (the maximum number of trials is set to 100 for possible failures). This process repeats until all chargers are placed or no further charger placement is possible. Besides, every point on curves of the algorithm stands for average value of 200 instances.

In contrast, the triangular placement algorithm follows the idea in [11]. Basically, this algorithm puts chargers at the end points of equilateral triangles. The side length of triangles is carefully determined such that the EMR safety is guaranteed, and some chargers will be randomly removed to meet the charger budget when necessary.

C. Performance Comparison

1) Impact of Threshold ϵ: Our algorithm's performance is mildly diminished as we increase the error threshold ϵ. As illustrated in Fig. 5, not surprisingly, the overall charging utility from all devices for the random algorithm and the triangular placement algorithm remains constant as ϵ rises from 0.65 to 0.85. In contrast, the charging utility for our PESA algorithm decreases by 22.5%. Note that, to reduce the running time of our algorithm, we set $\beta = 15$ and $D = 1.25$.

2) Impact of EMR Threshold R_t: Our algorithm outperforms the other algorithms by at least a factor of 45.7% as the EMR threshold R_t increases from 0.11 to 0.19. As depicted in Fig. 6, the charging utility of all three algorithms grows as R_t increases. Overall, our algorithm enjoys a performance gain of 103.1% over the random algorithm, and a gain of 45.7% over the triangular placement algorithm.

Besides, though the optimal solution is impossible to compute due to its extremely high computational cost, we can determine its upper bound by estimating the maximum possible charging utility for each device ($\frac{C_1}{C_2}R_t$) and adding them up ($\frac{C_1}{C_2}R_t m$). As a result, $(1-\epsilon)$ of the optimal solution to

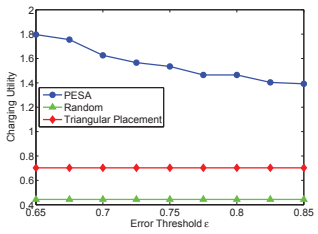

Fig. 5. Charging Utility vs. Error Threshold ϵ

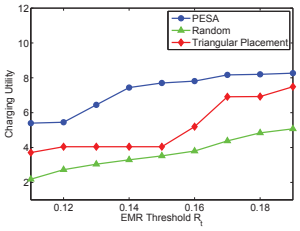

Fig. 6. Charging Utility vs. EMR Threshold R_t

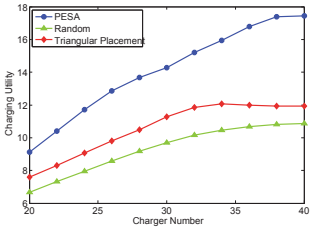

Fig. 7. Charging Utility vs. Charger Number

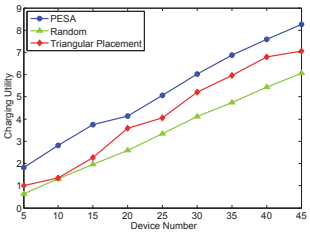

Fig. 8. Charging Utility vs. Device Number

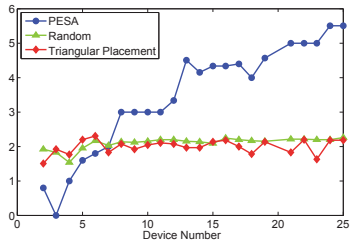

Fig. 9. Illustration of insight

PESA with a smaller EMR threshold $(1-\epsilon/2)R_t$ and a larger EMR radius $(1+\epsilon/2)D$ should be no more than $(1-\epsilon)(1-\epsilon/2)\frac{C_1}{C_2}R_t m$. Then we can use $U \geq (1-\epsilon)(1-\epsilon/2)\frac{C_1}{C_2}R_t m$ (U is the output of our algorithm) as a sufficient condition (but not a necessary condition) to check whether Theorem 3 holds or not. In this case, we have $(1-\epsilon)(1-\epsilon/2)\frac{C_1}{C_2}R_t m \leq 1.14$ and $U \geq 5.4$, which suggests the correctness of Theorem 3.

3) Impact of Charger Number: Our algorithm outperforms the other algorithms by at least a factor of 32.3% *as the number of chargers increases from* 20 *to* 40. As shown in Fig. 7, the charging utility of the two comparison algorithms first increases nearly linearly with the charger number. However, it then becomes relatively stable when the charger number is greater than 34. This is because the comparison algorithms are unable to deploy more chargers under the EMR safety constraint when the charger number exceeds 34, while our algorithm is more effective as it can still place more chargers to improve the performance. Moreover, the fact that $U \geq (1-\epsilon)(1-\epsilon/2)\frac{C_1}{C_2}R_t m$ also corroborates Theorem 3.

4) Impact of Device Number: Our algorithm outperforms the other algorithms by at least a factor of 39.4% *as the number of devices increases from* 5 *to* 45. Fig. 8 shows that the achieved charging utility of all three algorithms grows almost linearly with the device number. This is because when the devices are uniformly distributed, then the placement schemes for the three algorithms will not change too much as the device number increases, making the charging utility proportional to the device number. Again, the fact that $U \geq (1-\epsilon)(1-\epsilon/2)\frac{C_1}{C_2}R_t m$ supports Theorem 3.

D. Insights

In this subsection, we will explain why our algorithm can achieve a high charging gain. Suppose there are 100 devices distributed in a $20\,m * 20\,m$ field. The devices follow 2D Gaussian distribution with both x-coordinate and y-coordinate are randomly selected from a Gaussian distribution with $\mu = 10$ and $\sigma = 20/3$. The number of chargers to be placed is 30, error threshold $\epsilon = 0.8$, $R_t = 0.8$ and $D = 3$. We conduct three algorithms and for each output, we draw a disk centered at each device with radius D, and count the number of chargers and the number of devices covered by the disk. For a specific number of covered devices, we calculate the mean value of the covered chargers in the same disk (since there may be more than one disks cover the same number of devices), and plot the relationship between the number of covered devices and the corresponding average number of covered chargers in Fig. 9. We can see that the charger numbers of the random algorithm and the triangular placement algorithm remain nearly the same as the device number increases (about 2.07 and 2.08 respectively). Conversely, the charger number exhibits an increasing trend for our algorithm when the device number arises. It reaches 5.5 when the device number is larger than 24; note that in this case the charger density approaches the maximum allowed value under the EMR safety constraints. Thus, we conclude that for our algorithm, the placed number of chargers increases significantly with the density of devices. This will definitely lead to a larger charging utility than that of the comparison algorithms.

VII. Field Experiments

To better validate the correctness of our proposed scheme, we conduct field experiments in this section.

A. Experimental Setup

As depicted in Fig. 10, the indoor testbed consists of 5 TX91501 power transmitters produced by Powercast [2], 10 rechargeable sensor nodes, an AP connecting to a notebook to report the collected data from sensor nodes. Since the charging area of TX91501 power transmitters is roughly a sector with an angle $60°$ and a radius 4, we rotate them when necessary to mimic omnidirectional chargers. The coordinates of the 10 sensor nodes are $(1.40, 1.35)$, $(1.67, 1.40)$, $(2.33, 1.85)$, $(1.40, 2.05)$, $(1.33, 2.15)$, $(1.27, 2.35)$, $(1.47, 2.30)$, $(1.67, 2.20)$, $(1.70, 2.38)$ and $(1.80, 2.13)$, respectively. Besides, we suppose the placement area for chargers is shaped by the two dotted squares with side lengths 3.6 and 3.0, respectively, as shown in Fig. 10. Apparently, our algorithm, together with the random algorithm, can be directly extended to this case.

B. Experimental Results

The charger placement schemes for PESA and the random algorithm are demonstrated in Fig. 10. Generally, the PESA algorithm tends to put more chargers near to where nodes gather. Referring to Fig. 11, the overall charging utility for 10

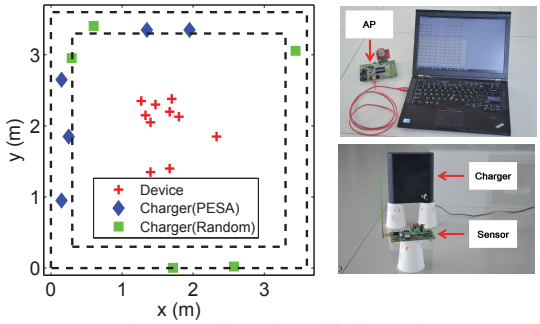

Fig. 10. Illustration of field experiment

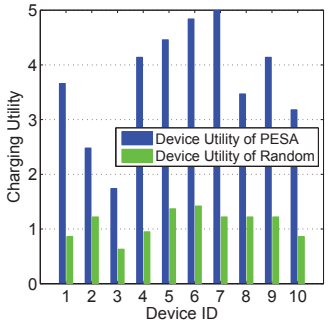

Fig. 11. Illustration of charging utility for PESA and the random algorithm

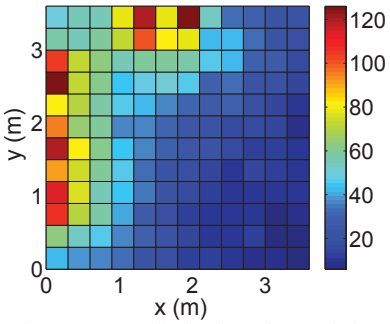

Fig. 12. EMR distribution of our solution

nodes of PESA outperforms that of the random algorithm by 70.5%, and the charging utility of PESA exhibits a greater variance than that of the random algorithm (the variances of the normalized charging utility of the two algorithms are 0.0426 and 0.0326, respectively). This can be ascribed to the fact that uniform charger distribution nature of the random algorithm would lead to uniform charging utility of devices. Note that we set $R_t = 140\,\mu W/cm^2$.

Fig. 12 shows the EMR distribution of our solution. It can be seen that even the maximum EMR on the plane, $126\,\mu W/cm^2$, is smaller than the established EMR threshold R_t. This observation corroborates the correctness of our algorithm.

VIII. Conclusions

This paper represents the first effort towards wireless charger placement with EMR safety. Other than the consideration of EMR safety, our work also advances the state-of-the-art on wireless charger placement from the following two fronts. First, in our work, chargers can be placed at any location on a discretized area and the discretization can be arbitrarily fine grained. This advantage helps us not only to find solutions that are close to the theoretically optimal solution, but also to analyze the approximation ratio of our solutions. Second, in our work, the wireless charging system achieves significantly better charging utility than prior art (by up to 45.7%).

Acknowledgment

The work is partly supported by China 973 projects (2014CB340303, 2012CB316201), China NSF grants (61502229, 61472184, 61321491, 61472252, 61133006, 61321491, 613220428, 613300260), the Jiangsu Future Internet Program under Grant Number BY2013095-4-08, the Jiangsu High-level Innovation and Entrepreneurship (Shuangchuang) Program, and the Shanghai Recruitment Program of Global Experts. Alex X. Liu is also affiliated with the Department of Computer Science and Engineering, Michigan State University, East Lansing, MI, USA.

References

[1] "http://www.seattle.intel-research.net/wisp/."
[2] "www.powercastco.com."
[3] M. OLTEANU, C. MARINCAS, and D. RAFIROIU, "Dangerous Temperature Increase from EM Radiation around Metallic Implants," *Acta Electrotehnica*, vol. 53, no. 2, 2012.
[4] M. P. Ntzouni, A. Skouroliakou, N. Kostomitsopoulos, and L. H. Margaritis, "Transient and cumulative memory impairments induced by gsm 1.8 ghz cell phone signal in a mouse model," *Electromagnetic biology and medicine*, 2013.
[5] M. Havas, J. Marrongelle, B. Pollner, E. Kelley, C. R. Rees, and L. Tully, "Provocation study using heart rate variability shows microwave radiation from 2.4 ghz cordless phone affects autonomic nervous system," *European Journal of Oncology Library*, vol. 5, 2010.
[6] M. J. Edwards, R. D. Saunders, and K. Shiota, "Effects of heat on embryos and foetuses." *International journal of hyperthermia: the official journal of European Society for Hyperthermic Oncology, North American Hyperthermia Group*, vol. 19, no. 3, pp. 295–324, 2002.
[7] O. P. Gandhi, L. L. Morgan, A. A. de Salles, Y.-Y. Han, R. B. Herberman, and D. L. Davis, "Exposure limits: The underestimation of absorbed cell phone radiation, especially in children," *Electromagnetic Biology and Medicine*, vol. 31, no. 1, pp. 34–51, 2012.
[8] "http://www.moh.gov.cn/zwgkzt/pgw/201212/34317.shtml."
[9] I. C. N. I. R. P. Guideline, "Guidelines for limiting exposure to time-varying electric, magnetic, and electromagnetic fields (up to 300 ghz). international commission on non-ionizing radiation protection." *Health Phys*, vol. 74, no. 4, pp. 494–522, 1998.
[10] H. Dai, Y. Liu, G. Chen, X. Wu, and T. He, "Safe charging for wireless power transfer," in *INFOCOM*, 2014.
[11] S. He, J. Chen, F. Jiang, D. K. Yau, G. Xing, and Y. Sun, "Energy provisioning in wireless rechargeable sensor networks," in *INFOCOM*, 2011.
[12] Y. Pang, Z. Lu, M. Pan, and W. W. Li, "Charging coverage for energy replenishment in wireless sensor networks," in *ICNSC*, 2014.
[13] S. Zhang, Z. Qian, F. Kong, J. Wu, and S. Lu, "P3: Joint Optimization of Charger Placement and Power Allocation for Wireless Power Transfer," in *INFOCOM*, 2015.
[14] H. Dai, Y. Liu, G. Chen, X. Wu, and T. He, "SCAPE: Safe Charging with Adjustable PowEr," in *ICDCS*, 2014.
[15] S. He, J. Chen, F. Jiang, D. K. Yau, G. Xing, and Y. Sun, "Energy provisioning in wireless rechargeable sensor networks," *IEEE Transactions on Mobile Computing*, vol. 12, no. 10, pp. 1931–1942, 2013.
[16] H. Dai, X. Wu, G. Chen, L. Xu, and S. Lin, "Minimizing the number of mobile chargers for large-scale wireless rechargeable sensor networks," *Computer Communications*, vol. 46, pp. 54–65, 2014.
[17] L. Fu, P. Cheng, Y. Gu, J. Chen, and T. He, "Minimizing charging delay in wireless rechargeable sensor networks," in *INFOCOM*. IEEE, 2013, pp. 2922–2930.
[18] H. Dai, G. Chen, C. Wang, S. Wang, X. Wu, and F. Wu, "Quality of energy provisioning for wireless power transfer," *IEEE Transactions on Parallel and Distributed Systems*, vol. 26, no. 2, pp. 527–537, 2015.
[19] A. L. Brearley, G. Mitra, and H. P. Williams, "Analysis of mathematical programming problems prior to applying the simplex algorithm," *Mathematical programming*, vol. 8, no. 1, pp. 54–83, 1975.
[20] R. J. Caron, J. F. McDonald, and C. M. Ponic, "A degenerate extreme point strategy for the classification of linear constraints as redundant or necessary," *Journal of Optimization Theory and Applications*, vol. 62, no. 2, pp. 225–237, 1989.
[21] S. Paulraj, C. Chellappan, and T. R. Natesan, "A heuristic approach for identification of redundant constraints in linear programming models," *International Journal of Computer Mathematics*, vol. 83, no. 8-9, pp. 675–683, 2006.
[22] A. Fréville, "The multidimensional 0–1 knapsack problem: An overview," *European Journal of Operational Research*, 2004.
[23] D.-Z. Du, K.-I. Ko, and X. Hu, *Design and analysis of approximation algorithms*. Springer, 2011, vol. 62.